An Optimized Equivalent Source Modeling for the Evaluation of Time Harmonic Radiated Fields from Electrical Machines and Drives

M. R. Barzegaran, Ali Sarikhani, and Osama A. Mohammed

Energy systems Research Laboratory, Department of Electrical and Computer Engineering
Florida International University, Miami, FL 33174, USA
mohammed@fiu.edu

Abstract ─ A model for electrical machines useful for radiated electromagnetic field studies in a multi-source environment is proposed. The various aspects of electromagnetic signature are considered. This model was created from a representative rectangular prism carrying a set of unbalanced currents in its branches. The geometry and the currents of the equivalent model were calculated based upon a genetic algorithm-based particle swarm optimization process taking into consideration the actual size and the operating conditions of the drive system being studied. The electric field was chosen as the objective function, which is the main element of the optimization. The simulated results show acceptable accuracy and excellent simulation time as compared to the full 3D FE model of the actual machine. Various types of signature studies of the model were conducted. This included stationary and time analysis in addition to the effect of rotation of the machine. For verification, we utilized two machines in a connected system to study and compare the results with their actual model. The results show satisfactory accuracy. The practical implication of this effort is in the fact that, with this equivalent model, we can evaluate radiation and stray effects for EMC evaluation at the design stage.

Index Terms ─ Electromagnetic field signatures, electric machines and drives, finite element analysis, optimization, and time harmonic field analysis.

I. INTRODUCTION

In the recent years, there has been an increased interest in the expansion of multi-level numerical simulation methods for investigation of EMI issue, in the early stages of the design of electrical apparatus at low frequency. Systems such as electric drives and power converters circuits are in this category of systems being studied. The EMI studies of a complete motor drive system were performed by several numbers of researchers [1-9]. In [1, 2], the kHz range frequency models of the various components of a complete motor drive were developed. The efforts have been made to measure the EMI emissions from kHz up to the GHz range in the case of adjustable speed drives (ASD). The EMI modeling and simulation for inverters were also performed. For EMI caused by the ground current in [3], the coupled FE-circuit high frequency electric machine model for simulating electromagnetic interference in a motor drive was presented. The model can predict the EMI caused by the ground current and motor terminal overvoltage. The proposed model in [2] can be used as a computational prototyping tool for evaluating the high frequency operating conditions of electric machines numerically. Likewise, studies in lower frequency are performed. For signature studies outside the machine, Le Coat *et al* evaluated electromagnetic signatures of induction machines [4]. Two types of these machines were studied experimentally and theoretically using 2D and 3D methods. The 3D model consists of several frames as conductors and specific frame with suitable permeability as stator. The results show that this model has good accuracy and is suitable for single machine case

Submitted On: Dec. 6, 2012
Accepted On: Feb. 10, 2013

1054-4887 © 2013 ACES

study. More similar works, in this area, were conducted by others [5-9].

In order to study the electric and magnetic behavior of power components in multi component study, an accurate physics-based model of each component is considered in this paper. For instance, all windings, type of connections in addition to the geometrical features slot shapes; rotor and stators structure as well as material properties are considered in developing the actual machine model.

In addition to the electric machines, other components such as power converters, cables and transformers have very tiny elements. Considering all of these in the FEA model causes an increase in the computational complexity. In addition to considering the essential elements of each parameter for the EMI study, there is a need to observe the fields in far distances. Therefore, a very large region must be considered in such a model. Therefore, the number of degrees of freedom in meshing will increase dramatically and subsequently the speed of analysis will decrease. Consequently, logical simplification in designing components should be implemented.

In this paper, it is proposed to develop the complete geometrical model of the machine to a simple rectangular prism but it should produce similar electromagnetic behaviors for studying the EMI issues. The basic concept for EMI signature evaluation for this case is explained in section II below. The study approach was investigated in section III for the purpose of simplifying the model of electrical machine. The optimization process and other theoretical aspects are explained in this part. The electric field is chosen as the objective function, which is the most important parameters in the optimization. The various aspects of the model including time analysis are also studied. Since it is proposed to use this model as a typical model for an induction machine, other operating conditions of this machine are investigated. For verification purposes, in all part of this study, the results of the model are compared with the result of the actual model.

II. BASIC CONCEPT

We are primarily interested in the radiation pattern of the electric component (in this case electrical machines) at a distance from the source. Hence, the electromagnetic fields are usually measured at a considerably far distance from the components. The electric and magnetic fields specifically at an infinite distance can be the most effective index in investigating the EMI [10]. Since the wave length in power frequency, 60 Hz, is so large, the far distance means thousand kilometers or more. Therefore, the region and proposed measurement points, which are intended to be far, should be considered in a very far distance. However, computationally utilizing such a large region could be impossible. Hence, we need to obtain the fields virtually. The process of obtaining the fields, in this case, is investigated. Figure1 shows the geometry for calculating the EMI from the motor at a far distance.

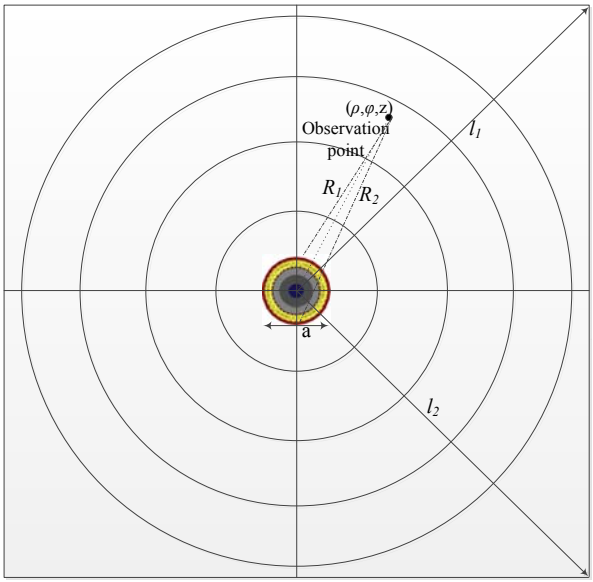

Fig. 1. Geometry for calculating the electromagnetic field at relatively far distances.

The present concept is based upon the Stratton-Chu [11] magnetic field intensity solution to the time-harmonic form of Maxwell's equations. The mathematical form used here, given by Silver [12, 13] yields the magnetic flux density as a volume integral of the electric and magnetic current densities, J and M, respectively,

$$\bar{B}(P) = \frac{-j}{4\pi\omega}\int_V [(\bar{M}.\bar{\nabla})\bar{\nabla} + k^2\bar{M} + j\omega\mu\bar{J}\times\bar{\nabla}].\frac{e^{-jkR}}{R}dV. \quad (1)$$

In the above equation, P denotes the observation point, V is the volume occupied by J and M. Here, R is the vector from the current

density elements J and M to the observation point P. Also, ω is equal to $2\pi f$ where f is the frequency of the currents. Finally, k is the wave number given by $k = \omega(\mu\varepsilon)^{1/2}$, where ε and μ are the permittivity and permeability of the medium, respectively. The time-harmonic variation $e^{j\omega t}$ has been suppressed.

It is assumed that the volumetric current density elements, $J\ dV$, can be represented as linear current elements $I\ dl$, located at infinity and aligned with the current flow directions. Recalling that M = 0, and completing the indicated vector operations yield,

$$\overline{B}(P) = \frac{\mu}{4\pi}\int_{l_1}^{l_2}\left[\left(jk + \frac{1}{\boldsymbol{R}}\right)\frac{e^{-jkR}}{R}\right].I(l)\left(\overline{dl}\times\overline{u_R}\right) \quad (2)$$

where u_R is the unit vector pointing in the direction of R. The bracketed term in equation (2) describes the time-harmonic retardation effects for the current element $I\ dl$, and suggests a criterion for using a quasi-static electromagnetic formulation. The l_1 and l_2 are considered the distance of the source to the end of the region to have the possibility of the calculation of the radiated B at any given P point in the area. The geometry is illustrated in Figure 1. Examining equation (2), it is seen that whenever,

$$R << \frac{c}{2\pi f}, \quad (3)$$

where c is the homogenous medium light speed, the bracketed term may be approximated by $1/\mathbf{R}^2$ and equation (2) reduces to the electromagnetic quasi-static result,

$$\overline{B}(P) \cong \frac{\mu}{4\pi}\sum_{i=1}^{2}\int_{l_1}^{l_2}\left[\frac{1}{\boldsymbol{R_i}^3}I_i(l)\right].\left(\overline{dl}_i\times\overline{R}_i\right)]. \quad (4)$$

In equation (4), the summation is over the two points of the source with I, being the currents in the motor wires, dl, the current elements along the motor wires, and R, the vectors from the current elements dl, to the observation point P (i = 1 and 2 for the corresponding points). Additionally, to facilitate computer programming, the vector R, is used in the cross product of equation (4). This is in contrast to the unit vector u_R, which was used in equation (2), resulting in R_i^3 in the integrand denominator of equation (4).

Returning to equation (4), the distances R_i between the differential line elements dl_i and the observation point, P, are (see Fig. 1),

$$R_1 = [\rho^2 + a^2 - 2\rho a\cos(\varphi - 2\pi z) + (Z - z)^2]^{1/2}, \quad (5)$$

$$R_2 = [\rho^2 + a^2 + 2\rho a\cos(\varphi - 2\pi z) + (Z - z)^2]^{1/2}, \quad (6)$$

where ρ, φ, and z are the cylindrical coordinates of the observation point and a is the width of the source. Assuming that the currents I_i, are oppositely directed, identical, and uniform over the length of the winding in the motor, substitution of the differential current elements dl_i and the distances R_i into equation (4) yields the Cartesian components of the magnetic flux density,

$$B_x = \frac{\mu I}{4\pi}\int_{z_1}^{z_2}\{\boldsymbol{R_1}^{-3}[2\pi a(Z-z)\cos(2\pi z) + a\sin(2\pi z) - \rho\sin(\varphi)] + R_2^{-3}[2\pi a(Z-z)\cos(2\pi z) + a\sin(2\pi z) + \rho\sin(\varphi)]\}dz, \quad (7)$$

$$B_y = \frac{\mu I}{4\pi}\int_{z_1}^{z_2}\{R_1^{-3}[2\pi a(Z-z)\sin(2\pi z) - a\cos(2\pi z) + \rho\cos(\varphi)] + R_2^{-3}[2\pi a(Z-z)\sin(2\pi z) - a\cos(2\pi z) - \rho\cos(\varphi)]\}dz, \quad (8)$$

$$B_z = \frac{\mu I}{4\pi}\int_{z_1}^{z_2}2\pi a\{R_1^{-3}\left[a - \rho\cos(\varphi - 2\pi z)\right] - R_2^{-3}[a + \rho\cos(\varphi - 2\pi z)]\}dz. \quad (9)$$

In the above equations, I is the total current in each wire of the motor in phase A, z_1, and z_2 are the axial coordinates of the electrical machine end points, and R_1 and R_2 are given by equations (5) and (6). According to standards, when ρ = 0, equations (7) to (9) reduce to the well-known expressions for the on-axis magnetic flux densities of motors in the region, [14, 15].

In order to derive the electric field as well as the magnetic field, with the spherical coordinate components of B known, the next step is straightforward [10]. The free space relationship shown in equation (10) is applied to equation (11),

$$H = \mu_0^{-1}B, \quad (10)$$

$$E = \frac{1}{j\omega\varepsilon_0}\nabla\times H. \quad (11)$$

The analysis method, which is used in this analysis, is the generalized minimal residual method (usually abbreviated GMRES) with successive over-relaxation (SOR) pre and post smoothers. The GMRES is an iterative method for the numerical solution of system of linear equations [16]. In numerical linear algebra, the SOR is a variant of the Gauss–Seidel method for solving a linear system of equations, resulting in faster convergence. The convergence is shown in Fig. 2. A similar method can be used for any slowly converging iterative process. The SOR method uses a more accurate approximation of the matrix, which leads to fewer iterations but slightly more work is required per iteration than in the Jacobi method. It should be noted that the problem consists of nonlinear equations due to the presence of the B-H curve of the core of the motor. The iterative solver solves the problem by dividing the nonlinear curves to the sets of linear one as μ_r ramp and solving each of them individually [16].

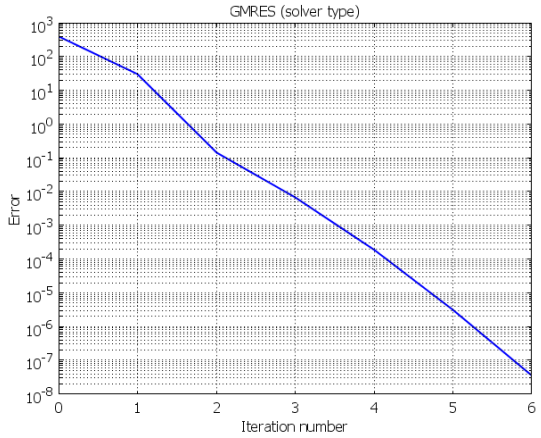

Fig. 2. Convergence of the problem using GMRES solver.

III. STUDY APPROACH

The electromagnetic signature study of the electrical machine in Figs. 1 and 3 (a) can be estimated based on equations (7) to (11). Since the electric and magnetic fields are interconnected to each other through equations (10) and (11), studying each of them shows the behavior of the electric machine at a far distance. However, as it is mentioned earlier, estimating the parameters of electrical machines at far distances requires significant time especially for multi-component studies using physics-based simulations. Therefore, a logical simplification was used here throughout the optimization.

The proposed equivalent machine model for signature study is a rectangular prism as shown in Fig. 3 (b). The cylinder around the model is for concentrating meshes to have accurate results. The rectangular prism model has currents in all of its branches, which are evaluated based upon an intelligent optimization process. The rectangular prism lengths (A, B, C) and the corresponding currents to each leg (i_{x1} i_{x2} i_{x3} i_{x4}, i_{y1} i_{y2} i_{y3} i_{y4}, and i_{z1} i_{z2} i_{z3} i_{z4}) are calculated. The proposed optimization process (GA-based PSO) is explained next.

PSO is a population-based algorithm that exploits a population of individuals to probe promising region of the search space. In this context, the population is called swarm and the individuals are called particles. Each particle moves with an adaptable velocity within the search space and retains in its memory the best position it ever encountered. The global variant of PSO, the best position ever attained by all individuals of the swarm is communicated to all the particles. The general principles for the GA and the PSO algorithms are stated in [17].

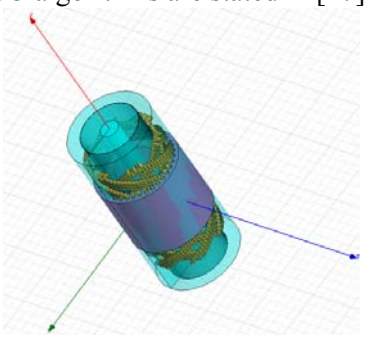

(a)

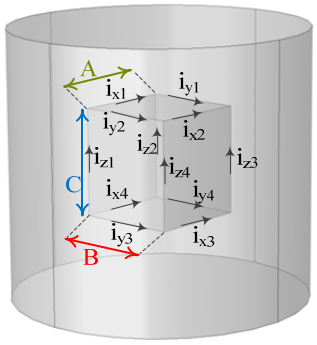

(b)

Fig. 3. Prototype of the proposed machine (SCIM) in finite element analysis for (a) actual model and (b) an equivalent current loop model for signature studies.

In order to prevent premature convergence to suboptimal solutions, Raymond Tan augmented a binary PSO with a GA-based mutation operator and achieved significant improvement in the rate of successful convergence [18]. Therefore, in the current study we incorporated a mutation operator into our continuous-space PSO algorithm. This mutation operator reinitiates the value of each continuous variable into its feasible range by a predefined probability (e.g., 5 %).

In this study, the number of population is set to 7, and for preventing explosion of the swarm, the maximum allowable velocity along each dimension is set to half of its feasible ranges. The results show that, in this application, for different number of switching angles, the algorithm converges within 100 to 150 iterations. Hence, in a conservative manner, the number of iterations is set to 30. Also, for enhancing the PSO's ability in escaping from local minima, a mutation operator is incorporated into the algorithm. The results indicate that, it is better to utilize this operator in discrete iteration intervals, with different probability. In this study, the mutation probabilities for iteration intervals of {5, 7} and {7, 30} are 1 % and 3 %, respectively. Other iteration intervals are not influenced by mutation.

The objective function of the optimization process for this case is the main index for evaluating the values of the model. This is because the initial and the later in the process, the modified values are just compared by means of the objective function. For this paper as mentioned earlier, the electric field was chosen, which is because of sensitivity of electric field in signature studies. In other words, the effect of changes on the condition of the component has influence on the electric field [19]. Consequently, the objective function is assigned as follows,

$$obj = mean(|Ex_{motor}| - |Ex_{rp}| + |Ey_{motor}| - |Ey_{rp}| + |Ez_{motor}| - |Ez_{rp}|). \quad (12)$$

where *E*x, *E*y, and *E*z represent the normal electric field along a line in *x*, *y*, and *z* directions. The indices, *motor* and *rp* stands for actual 3D motor model, and its correspondence to the rectangular prism current loop model (see Fig. 3).

IV. SIMULATION APPROACH

In this study, the finite element analysis is used as an accurate method for physics-based simulation. The analysis of electromagnetic finite element method is based on equation (13) and typical Maxwell equations,

$$\nabla \times \mathbf{H} = \mathbf{J} = \sigma(\mathbf{E} + \mathbf{v} \times \mathbf{B}) + \mathbf{J}^e \quad (13)$$

where $\mathbf{J}^e$ is an externally generated current density and $\mathbf{v}$ is the velocity of the conductor. Note that $\mathbf{B}$ and $\mathbf{E}$ are used uniquely in magnetic or electric solution, respectively, but are fully coupled here.

Using the definitions of the fields $\mathbf{B} = \nabla \times \mathbf{A}$ and $\mathrm{E} = -\nabla V - j\omega\mathbf{A}$ and combining them with the constitutive relationships $\mathbf{B} = \mu_0(\mathbf{H} + \mathrm{M})$ and $D = \varepsilon_0\mathbf{E}$ and rewriting Ampere's law, the required current density will be achieved,

$$\begin{aligned}&(j\omega\sigma - \omega^2\varepsilon_0)\mathbf{A} + \nabla \times (\mu_0^{-1}\nabla \times \mathbf{A} - \mathbf{M}) \\ &-\sigma\mathbf{v} \times (\nabla \times \mathbf{A}) + (\sigma + j\omega\varepsilon_0)\nabla V = \mathbf{J}^e.\end{aligned} \quad (14)$$

The equation of continuity is obtained by taking the divergence of Ampere's law. This equation is solved for the electric potential. Thus the following equations for V and A is obtained,

$$\begin{aligned}&-\nabla.\Big((j\omega\sigma - \omega^2\varepsilon_0)\mathbf{A} - \sigma\mathbf{v} \times (\nabla \times \mathbf{A}) \\ &+(\sigma + j\omega\varepsilon_0)\nabla V - (\mathbf{J}^e + j\omega\mathbf{P})\Big) = 0.\end{aligned} \quad (15)$$

A particular gauge can be obtained by reducing the system of equation by choosing $\Psi = -jV/\omega$ in the gauge transformation. Therefore, the modified magnetic vector potential is obtained as

$$\tilde{\mathbf{A}} = \mathbf{A} - \frac{j}{\omega}\nabla V. \quad (16)$$

Working with $\tilde{\mathbf{A}}$ is often the best option when it is possible to specify all source currents as external currents $\mathbf{J}^e$ or as surface currents on boundaries,

$$\begin{aligned}&\left(j\omega\sigma - \omega^2\varepsilon_0\right)\tilde{\mathbf{A}} + \nabla \times \left(\mu_0^{-1}\nabla \times \tilde{\mathbf{A}} - \mathbf{M}\right) - \\ &\sigma\mathbf{v} \times \left(\nabla \times \tilde{\mathbf{A}}\right) + \left(\sigma + j\omega\varepsilon_0\right)\nabla V = \mathbf{J}^e + j\omega\mathbf{P},\end{aligned} \quad (17)$$

where $\mathbf{A}$ is magnetic potential, $\mathbf{J}^e$ is external current density, $\mathbf{M}$ is magnetization and $\mathbf{v}$ is the motion speed, which here, it is equal to zero. Equation (17) is a modified version of the classic quasi-static equation (15), which is implemented in the FE software. The magnetic field density ($\mathbf{B}$)

for the evaluation of the radiated field would be calculated by getting **A** from equation (17) and applying it to $\mathbf{B} = \nabla \times \mathbf{A}$.

Further modification in this study is applied by linking Matlab software with FE software. This can be done by defining a variable in Matlab codes as **D** (electric displacement field) and making a link to the FE software, then considering this new **D** instead of the default D. This new defined electric displacement field is based on the electric field obtained from the software solution. The other element ($\tilde{\mathbf{A}}$) is defined in the same way.

V. SIMULATION RESULT AND DISCUSSION

For simulation purposes, a 3-phase, 380-V, 5-A, 120-turn/phase induction machine with stack length of 0.15 m and outer diameter of 17.5 cm is simulated in the 3D electromagnetic FE domain for one instant of time at the frequency of 60 Hz. The electric field along three lines in the *x*, *y*, and *z* directions are calculated. The optimization process was then implemented.

Following the optimization process, the rectangular prism length are calculated as (A = 0.1009 m, B = 0.125 m, C = 0.1282 m). Table 1 shows the calculated current for the rectangular prism branches following the optimization process in one case. Although the optimization is performed with the electric field as the objective function, the magnetic field radiated form the proposed model also shows great similarity when it compares with actual model.

Table 1: The calculated current for rectangular prism legs.

i_{x1}	i_{x2}	i_{x3}	i_{x4}
-61.18	528.12	-267.44	-107.82
i_{y1}	i_{y2}	i_{y3}	i_{y4}
-115.25	-251.54	36.107	424.1
i_{z1}	i_{z2}	i_{z3}	i_{z4}
-150.03	-99.84	4.46	-135.6

The comparison between the normal electric field of the actual 3D model and the cubic model for one motor case is illustrated in various circumstances. For brevity, only some indices including field spectrum, arrow-line and stream-line are selected for the study. For instance, electric field spectrum radiated from the actual machine and the equivalent models are compared as shown in Fig. 4. Also, magnetic field density spectrum was compared and is shown in Fig. 5. The magnetic field density is evaluated with the same amount of current shown in Table 1 for this specific case.

Considering Fig. 4, the accuracy of the E field in all coordinates is significantly similar as the difference between the two models, which is really negligible. By choosing different optimization parameters including; mutation probabilities, iteration intervals, and number of iteration, the inaccuracy of the equivalent model in some points can be fixed. As shown in Figs. 4 and 5, the electromagnetic fields radiate dipole fields at far distance because the machine will act similar to a complex loop and a loop will propagate dipole electromagnetic fields.

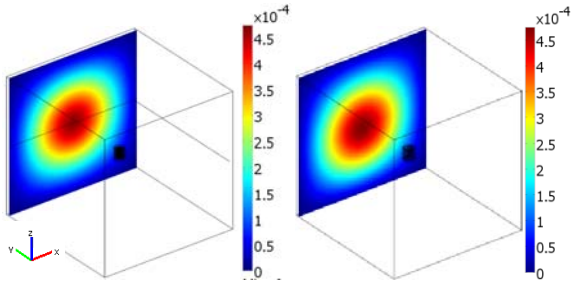

(a) (b)

Fig. 4. Electric ield spectrum (V/m) of (a) actual machine and (b) equivalent source model in the *xz*-plane.

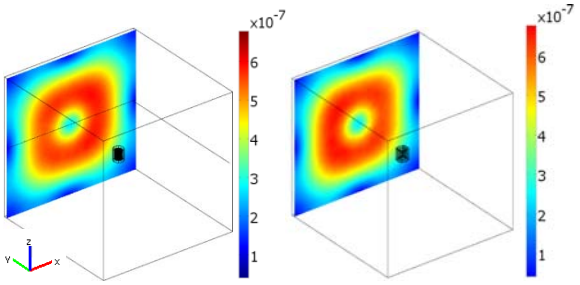

(a) (b)

Fig. 5. Magnetic field density spectrum (T) of (a) actual machine and (b) equivalent source model in the *xz*-plane.

The figure shows that with the amount of current in Table 1, the equivalent model has similar electromagnetic behavior to the actual machine as the signature study point of view. In addition to the importance of the accuracy of the field spectrums, the direction of the flowing fields is significant because the field spectrum figures, Figs. 4 and 5, don't show the direction of the fields. Hence, the arrow line of magnetic field density of the actual and equivalent machines are compared and shown in Fig. 6. As displayed in this figure, the magnetic field in the actual case around the motor is denser in comparison with the equivalent source model case. However, the radiated magnetic field at further distance is almost the same in these two models. This is more important because the model is designed for far distance. While the arrow plot in Fig. 6 shows the magnetic field density, this can be classified as discrete streamline of this field. A continues stream-line of the H field (magnetic field intensity) of the two models (actual and equivalent source models) is obtained as shown in Fig. 7. The H field streamline also shows that the equivalent source model has very similar result to the actual model. It also shows that the dipoles establish around the equivalent source model also in near distance. It should be noted that the purpose of this model was to obtain resembling fields at far distance.

For other conditions of the machine; for example other voltages or power rates and/or other size of the machine, the ratio of the new condition to a basic condition can be considered. The basic case could be any case similar to the case studied in this paper. Then this ratio will be applied to the currents. It is likely to have similar results compared to the actual case in the new condition. As mentioned earlier in the paper, the main goal of this research is to study the signature of multi machine system. For validation of the calculated equivalent source model (rectangular prism) from one motor case, the model is compared in a case containing two motors, as shown in Fig. 8, while the current in the branches of the rectangular prism model remain the same as in the first case. The centers of the coordinates of the two rectangular prisms are exactly the same as the 3D motor model. The figure shows a comparison between the electric field spectrum in the actual and rectangular prism model for the two motor cases. As can be seen, the electric fields similarly follow the same patterns with acceptable accuracy. Also magnetic field density, which is shown in Fig. 9 has a very good accuracy in comparison with the actual model.

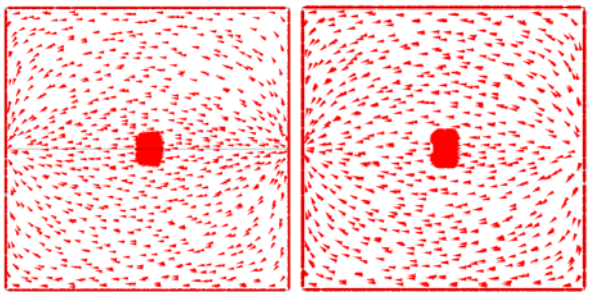

(a) (b)

Fig. 6. Arrow plot of magnetic field density (T) of (a) actual machine and (b) equivalent model in the *xy*-plane.

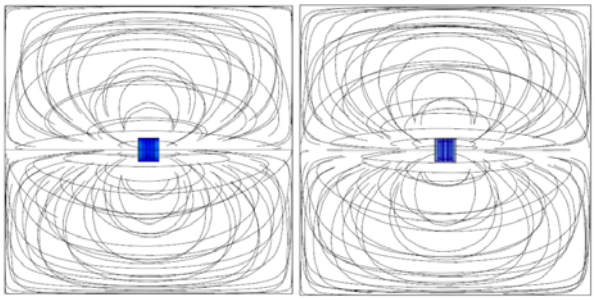

(a) (b)

Fig. 7. Stream-line of H field of (a) actual machine model in the *xy*-plane (A/m) and (b) equivalent source model in the *xy*-plane (A/m).

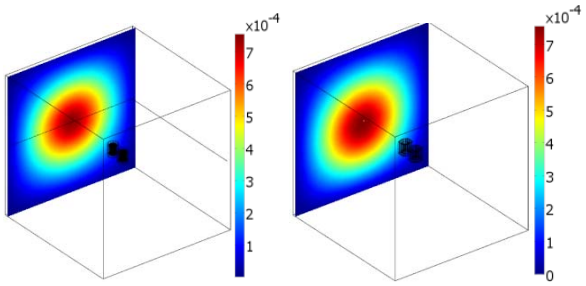

(a) (b)

Fig. 8. Electric field spectrum (V/m) of (a) actual machine and (b) equivalent source model in the *xz*-plane in the two machine case.

A. Simulation time comparison

Comparison between the simulation time of the actual model and equivalent model shows that this approach makes the simulation at least 100 times faster than the full 3D model. This enables the numerical simulation of multiple sources in a reasonable time allowing the practical study of EMC issues during electric drive development stages. Moreover, it is observed that in case of evaluation of the field in some directions more accurate results can be calculated.

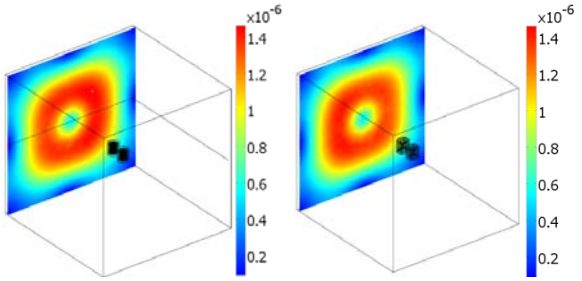

(a) (b)

Fig. 9. Magnetic field density (T) spectrum of (a) actual machine and (b) equivalent model in the *xz*-plane in the two machine case.

VI. TIME AND ROTATION STUDY

A. Time-based analysis

Since the actual induction machine carries AC current, the time-based analysis is more useful. Although in the previous sections, the analysis was time-based however, the figures are just depicted in one typical moment of time. In this section, the radiated electromagnetic fields of different instances of time in one cycle are studied. For brevity, four time instances are selected (0.0025 s, 0.005 s, 0.0075 s, and 0.0125 s). The voltage amplitude of the terminal of the model during one time cycle is shown in Fig. 10.

Firstly, the radiated magnetic field in the near distance (0.5 m) from the machine is studied. The magnetic field density measured in four time instants is shown in Fig. 11. The result shows that the magnetic field rotates by the variation in time, although the position of the maximum field point remained unchanged. It can be inferred from this result that the model resembles the machine and can be used instead of that at all time instants not just one time instant in which the model is designed. Next, the radiated magnetic field at a far distance (~10 m) from the machine is studied. In this distance the rule of the magnetic dipoles for these distances cause the field become similar to a dipole as shown in Fig. 12 [20]. As shown in this figure, the dipoles are sensitive to time changes and they rotates when the time changes. Consequently, the equivalent source model can be used for the time-based analysis at near and far distances.

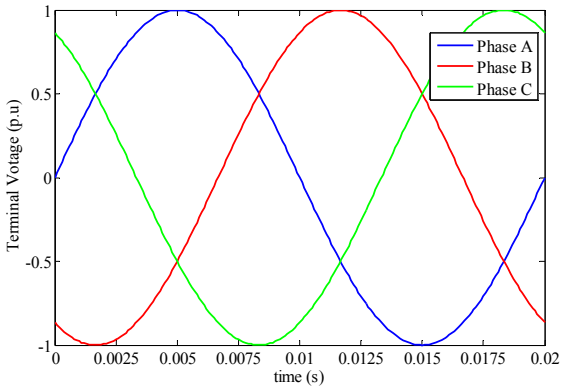

Fig. 10. Voltage amplitude of the terminal of the model during one time cycle.

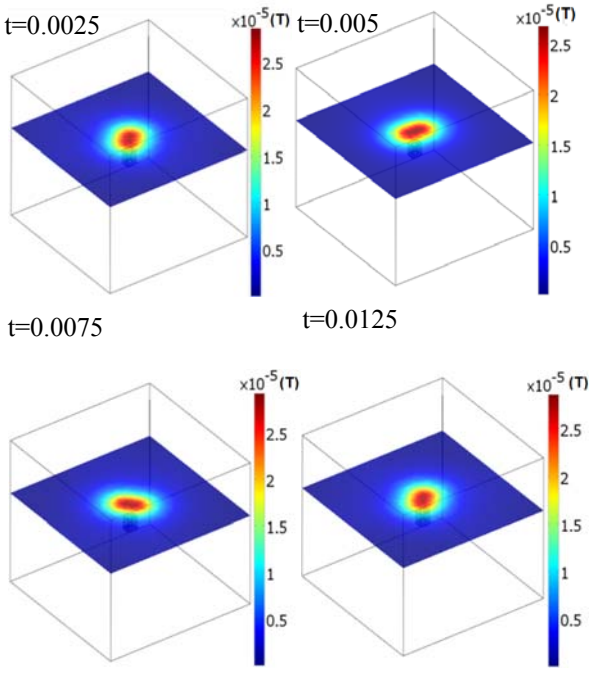

Fig. 11. Magnetic field density (B) of equivalent model in four different moments of time at near distance.

B. The effect of rotation

Another condition that should be studied for the induction machine is testing various positions of the machine. In many cases, the location of the motor with respect to the measured points will change. Therefore, the electromagnetic signatures are expected to be changed. Hence, a specific change of the motor is studied here. The whole machine was rotated around an axis and the results were obtained and illustrated in Fig. 13. The magnetic field in this figure is plotted at a far distance.

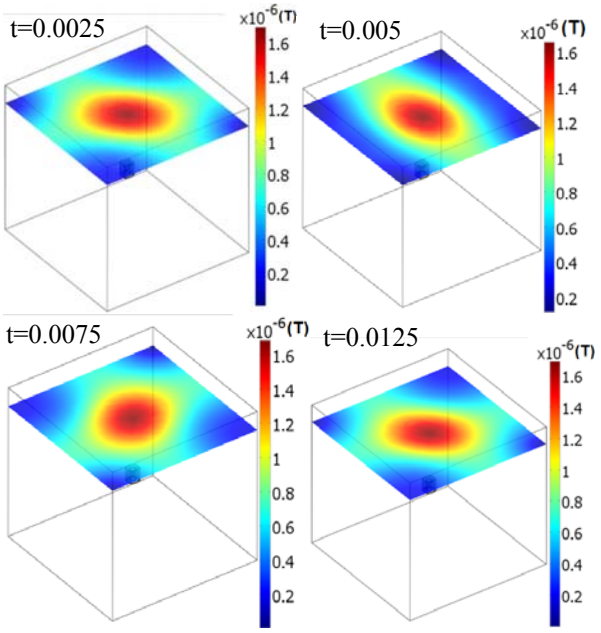

Fig. 12. Magnetic field density (B) of equivalent model at the four different intendances of time at far distance.

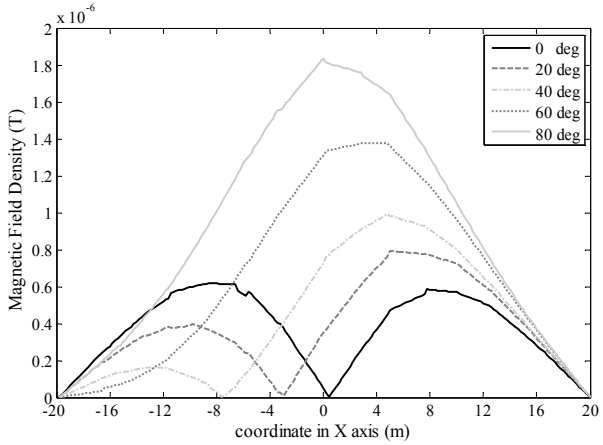

Fig. 13. Deviation of magnetic field density (B) of the equivalent model due to the rotation of the whole machine around z-axis.

As shown in Fig. 13, by rotating the stator of the induction machine around the z-axis, the magnetic field moves along the perpendicular coordinates (x, y) from right to left. When plotting other angles ranging from 90 to 180 degrees, the results are exactly symmetrical with respect to the changes from 0 to 90 degrees. The magnetic field density of 180 degree change is exactly the same as the one with 0 degree change. This study is useful in identifying the situation of the source machine by looking at the signatures at far distance. All of these studies can be imported to an optimization program such as genetic algorithm or neural network. Therefore, the machine in any situation can be recognized.

VII. CONCLUSION

Considering the simulation of multi-machine environment with actual models requires significant time and large computing resources. An equivalent source model for these electric machines for the purpose of evaluation signatures and radiated fields are designed, presented, and verified. A rectangular prism model was proposed with variable currents in its branches. The GA-based PSO method was used for evaluating the currents of the rectangular prism branches while the electric field was chosen as objective function because of its sensitivity to the change of situation. A modified finite element analysis was used, which include modification in the equations in which deviation of electric displacement field over time was considered. The accuracy of the results shows that it is possible to replace the actual model of the electrical machines with the equivalent rectangular prism current model for signature studies. The simulation time of the equivalent source rectangular prism model is approximately 100 times less than the actual model enabling the numerical simulation of multiple cases.

The model was validated by considering a two machine case as a representative situation of multi machine case. The actual models in two machine case were replaced with equivalent models in the sample position with the same values of single machine cases. The results show excellent accuracy with considerable simulation time reduction. This facilitates the numerical simulation of multiple electromagnetic sources in a reasonable time allowing the practical study of

important issues such as EMC standards during the development stages of electric drives systems. Furthermore, time harmonic analysis and the effect of rotation were investigated. These types of studies are useful in recognizing the condition of the source machine by looking at its signatures at a far distance.

REFERENCES

[1] O. A. Mohammed and S. Ganu, "FE-circuit coupled model of electric machines for simulation and evaluation of EMI issues in motor drives," *IEEE Transactions on Magnetics,* vol. 46, no. 8, pp. 3389-3392, Aug. 2010.

[2] O. A. Mohammed, S. Ganu, N. Abed, S. Liu, and Z. Liu, "High frequency phase variable model of electric machines from electromagnetic field computation," *Appl. Comp. Electro. Society (ACES) Journal*, vol. 22, no. 1, pp. 164-171, Mar. 2007.

[3] A. Rosales, A. Sarikhani, and O. A. Mohammed, "Evaluation of radiated electromagnetic field interference due to frequency switching in PWM motor drives by 3D finite elements," *IEEE Transactions on Magnetics*, vol. 47, no. 5, pp. 1474-1477, May 2011.

[4] G. Coat, A. Foggia, JP. Bongiraud, and P. Thiec, "Electromagnetic signature of induction machines," *IEEE Transaction on Energy Conversion,* vol. 14, no. 3, pp. 628-632, Sep. 1999.

[5] H. Hasper, "Reduction of magnetic stray field from squirrel-cage induction motors," *COMBIMAC document*, Feb. 1991.

[6] X. Brunotte, G. Meunier, and J. P. Bongiraud, "Ship magnetizations modeling by the finite element method," *IEEE Transactions on Magnetics*, vol. 29, no. 2, pp. 1970-1975, Mar. 1993.

[7] G. G. Karady, Sh. FI. Berisha, J. A. Demcko, and M. Samotyj, "Variable speed motor drive generated magnetic fields," *IEEE Transactions on Power Delivery*, vol. 9, no. 3, pp. 1639-1646, July 1994.

[8] A. Sarikhani and O. A. Mohammed, "Coupled electromagnetic field computation with external circuit for the evaluation the performance of electric motor designs," *Appl. Comp. Electro. Society (ACES) Journal*, vol. 26, no. 12, pp. 997-1006, Dec. 2011.

[9] J. H. Alwash and L. J. Qaseer, "Three-dimension finite element analysis of a helical motion induction motor," *Appl. Comp. Electro. Society, (ACES) Journal*, vol. 25, no. 8, pp. 703-712, Aug. 2010.

[10] F. Ulaby, *Fundamental of Applied Electromagnetics*, 5th Edition, Prentice Hall, Massachusetts, pp. 321-324, 2006.

[11] J. A. Stratton and L. J. Chu, "Diffraction theory of electromagnetic waves," *Physical Review*, vol. 56, pp. 99-107, 1939.

[12] S. Silver, *Microwave Antenna Theory and Design*. McGraw-Hill, 1949, MIT Rad. Lab. Series, vol. 12, Ch. 3, reprinted by Peter Peregrinus Ltd., London, UK, 1986.

[13] G. R. Piper and A. Prata, "Magnetic flux density produced by finite-length twisted-wire pairs," *IEEE Transactions on Electromagnetic Compatibility,* vol. 38, no. 1, pp. 84-92, Feb. 1996.

[14] W. R. Smythe, *Static and Dynamic Electricity*, vol. 28, McGraw-Hill, New York, pp. 296-298, 1968.

[15] J. G. Van Bladel, *Electromagnetic Fields*, vol. 19, John Wiley & Sons, New York, pp. 157, 1985.

[16] Y. Saad, *Iterative Methods for Sparse Linear Systems*, 2nd edition, Society for Industrial and Applied Mathematics, 2003.

[17] C. –F. Juang, "A hybrid of genetic algorithm and particle swarm optimization for recurrent network design," *IEEE Transactions on Cybernetics, Systems, Man, and Cybernetics, Part B,* vol. 34, no. 2, pp. 997-1006, Apr. 2004.

[18] R. Raymond, "Hybrid evolutionary computation for the development of pollution prevention and control strategies," *Journal of Cleaner Prod.*, vol. 15, no. 10, pp. 902-906, 2007.

[19] J. William, Y. Pan, E. J. Fenyves, I. Sujisawa, H. Suyama, N. Samadi, and G. H. Ross, "Electromagnetic field sensitivity," *Electromagnetic Biology and Medicine*, vol. 10, no. 1-2, pp. 241-256, 1991.

[20] T. L. Chow, *Introduction to Electromagnetic Theory: A Modern Perspective*, Jones & Bartlett Learning, Massachusetts, 2006.

Mohammadreza Barzegaran obtained B.Sc. and M.Sc. Degrees in Power Engineering from University of Mazandaran, Iran in 2007 and 2010, respectively. He is currently pursuing the Ph.D. degree in the department of Electrical and Computer Engineering, Florida International University, Florida, USA. His research interests include studying electromagnetic compatibility in power components, life assessment of electrical power components, fault detection in electrical machines, and also computer-aid simulation of power components. He has many published papers in international journals and conferences.

Ali Sarikhani received his Bachelor degree in Transmission and Distribution Engineering in Power and Water University of Technology, Iran. He followed his Masters in Power Electrical Engineering in Shahrood University of Technology, Iran. He is now a Ph.D. Candidate of Electrical Engineering at Energy Systems Research Lab, Florida International University, USA. His current interests are computational design prototyping, computational electromagnetic, and fault tolerant machine-drive systems.

Osama A. Mohammed (S'79, M'83 SM'84, F'94): is a Professor of Electrical and Computer Engineering and the Director of the Energy Systems Research Laboratory at Florida International University. He received his M.S. and Ph.D. degrees in Electrical Engineering from Virginia Polytechnic Institute and State University. He published numerous journal articles over the past 30 years in areas relating to power systems, electric machines and drives, computational electromagnetics and in design optimization of electromagnetic devices, artificial intelligence applications to energy systems. He authored and co-authored more than 350 technical papers in the archival literature. He has conducted research work for government and research laboratories in shipboard power conversion systems and integrated motor drives. He is also interested in the application communication and wide area networks for the distributed control of smart power grids. He has been successful in obtaining a number of research contracts and grants from industries and Federal government agencies for projects related to these areas. Professor Mohammed also published several book chapters including; Chapter 8 on direct current machinery in the Standard Handbook for Electrical Engineers, 15th Edition, McGraw-Hill, 2007 and a book Chapter entitled " Optimal Design of Magnetostatic Devices: the genetic Algorithm Approach and System Optimization Strategies," in the Book entitled: Electromagnetic Optimization by Genetic Algorithms, John Wiley & Sons, 1999.

Professor Mohammed is a Fellow of IEEE and is the recipient of the IEEE PES 2010 Cyril Veinott Electromechanical Energy Conversion Award. Dr. Mohammed is also a Fellow of the Applied Computational Electromagnetic Society. He is Editor of IEEE Transactions on Energy Conversion, IEEE Transactions on Magnetics, IEEE Transactions on Smart Grid and COMPEL. Professor Mohammed was the past President of the Applied Computational Electromagnetic Society (ACES). He received many awards for excellence in research, teaching and service to the profession and has delivered numerous invited lectures at scientific organizations around the world.

Professor Mohammed has been the general chair of several international conferences including; ACES 2006, IEEE-CEFC 2006, IEEE-IEMDC 2009, IEEE-ISAP 1996 and COMPUMAG-1993. He has also chaired technical programs for other major international conferences including; IEEE-CEFC 2010, IEEE-CEFC-2000 and the 2004 IEEE Nanoscale Devices and System Integration. Dr. Mohammed also organized and taught many short courses on power systems, Electromagnetics and intelligent systems in the U.S.A and abroad. Professor Mohammed has served ACES in various capacities for many years. He also serves IEEE in various Boards, committees and working groups at the national and international levels.